

Prokaryotic community temporal variation in a coastal marine environment

Marino Korlević^{1*}, Marsej Markovski¹, Gerhard J. Herndl^{2,3} and Mirjana Najdek¹

1. Center for Marine Research, Ruđer Bošković Institute, Croatia

2. Department of Functional and Evolutionary Ecology, University of Vienna, Austria

3. NIOZ, Department of Marine Microbiology and Biogeochemistry, Royal Netherlands Institute for Sea Research, Utrecht University, The Netherlands

*To whom correspondence should be addressed:

Marino Korlević

G. Paliaga 5, 52210 Rovinj, Croatia

Tel.: +385 52 804 768

Fax: +385 52 804 780

e-mail: marino.korlevic@irb.hr

Running title: Temporal variation of a coastal prokaryotic community

1 Abstract

2 Prokaryotic communities inhabiting surface waters of temperate areas exhibit patterns of
3 seasonal succession. Studies describing these temporal changes were usually not performed at
4 stations located in the proximity of the coast. The temporal variation of these communities was
5 determined in the northern Adriatic Sea surface waters sampled at two stations located in the close
6 proximity of its western shore. Sequencing of the V4 region of the 16S rRNA gene identified a
7 community richness maximum in December and a temporal exchange of a spring, summer and
8 autumn/winter-specific community. Temperature was shown to be the main environmental force
9 explaining community temporal variation. Taxonomic analysis determined low-level taxa present
10 throughout the year and groups specific to each identified temporal community. The *Synechococcus*,
11 SAR86 clade, NS5 marine group and *Cryomorphaceae* were detected through the year. In contrast,
12 the spring community was characterized by the NS4 marine group, *Formosa* and *Rhodobacteraceae*,
13 the summer community by SAR11 subclades II and III, HIMB11, AEGEAN-169 marine group,
14 OM60 (NOR5) clade and *Litoricola* and the autumn/winter community by SAR11 subclade Ia
15 and *Archaea*. Taken together, prokaryotic communities inhabiting coastal surface waters exhibit
16 general phenomena similar to other surface associated assemblages, but are also characterized by
17 season-specific community structures and temporal patterns of certain taxonomic groups that differ
18 from other areas.

19 **Introduction**

20 Prokaryotic picoplankton communities inhabiting marine surface waters exhibit patterns of
21 seasonal succession. These temporal community changes were described for surface waters of polar,
22 temperate and (sub)tropical regions (Bunse and Pinhassi, 2017). In temperate regions changes were
23 mainly associated with summer water column stratification, winter mixing and spring phytoplankton
24 blooms (Teeling et al., 2012; Bunse and Pinhassi, 2017; Mestre et al., 2020). Although general
25 successional patterns in these waters were reported, some local differences were also observed.
26 While some studies have reported the exchange of multiple community states during the year
27 (Gilbert et al., 2009; Sintes et al., 2013; El-Swais et al., 2015; Lindh et al., 2015), others have
28 observed a community separation in only two major groups (Mestre et al., 2020), indicating that
29 beside global patterns local environmental conditions may influence seasonal community change.

30 Seasonal community variation in temperate waters usually starts with assemblages
31 characteristic for spring phytoplankton blooms. The successional pattern of different microbial
32 groups during the pre-bloom, bloom and bloom-decay periods have been described in detail
33 (Teeling et al., 2012, 2016; Sintes et al., 2013). The pre-bloom community is generally dominated
34 by members of the alphaproteobacterial SAR11 clade, during the bloom *Bacteroidota* taxa such as
35 *Formosa*, *Polaribacter*, *Ulvibacter* and the VIS6 clade become abundant while the decay period is
36 characterized by *Gammaproteobacteria*, i.e. the SAR92 clade (Teeling et al., 2012, 2016; Sintes
37 et al., 2013). Beside taxa co-occurring with phytoplankton blooms, communities specific to
38 summer water stratification and winter mixing were also described (Mestre et al., 2020). Usually,
39 *Cyanobacteria* are enriched during summer periods, while the SAR11 clade exhibit an interesting
40 trend with some sub-clades being characteristic for summer and some for winter months (Salter et
41 al., 2015; Mestre et al., 2020).

42 The majority of studies describing temporal changes in temperate areas were performed at
43 long-term time series locations, such as the L4 sampling site of the Western Channel Observatory

44 (Gilbert et al., 2009, 2012), Blanes Bay Microbial Observatory (BBMO) (Alonso-Sáez et al., 2007;
45 Mestre et al., 2020), Linnaeus Microbial Observatory (Lindh et al., 2015), station Kabeltonne in the
46 German Bight (Teeling et al., 2012, 2016) and station E2 of the RADIALES time-series project
47 (Alonso-Sáez et al., 2015). Data obtained from such time-series studies have found that a set of
48 abiotic and biotic factors drive the temporal community variation (Bunse and Pinhassi, 2017). It
49 was suggested that biological interactions primarily affect microbial dynamics over shorter time
50 periods of days to weeks, while physicochemical parameters are mainly responsible for observed
51 seasonal successional patterns (Gilbert et al., 2009; Fuhrman et al., 2015; Needham and Fuhrman,
52 2016; Bunse and Pinhassi, 2017; Mestre et al., 2020). In addition, several studies indicate that
53 the phytoplankton derived dissolved organic matter (DOM) indirectly drives community dynamics
54 (Teeling et al., 2012, 2016; Lindh et al., 2015; Needham and Fuhrman, 2016; Bunse and Pinhassi,
55 2017). It is therefore worth investigating if such general such general interactions also apply to
56 coastal microbial communities inhabiting the proximity of the shore.

57 To describe the temporal variation of microbial communities in ecosystems located in the
58 proximity of the shore and to disentangle the environmental variables responsible for their temporal
59 change it is important to apply a high-frequency sampling approach. In order to determine the
60 temporal variation of prokaryotic picoplankton communities in these habitats monthly sampling of
61 surface waters at two stations along the western coast of the northern Adriatic Sea was performed.
62 In addition, to assess the main environmental parameters associated with community changes
63 compositional data were constrained by a set of previously reported environmental parameters
64 measured at the same time (Najdek et al., 2020a, 2020b).

65 **Materials and methods**

66 **Sampling**

67 Surface seawater from the northern Adriatic Sea was collected in the proximity of the coast
68 (25 – 50 m) in two closely located bays (~7 km apart), Saline (45°7'5" N, 13°37'20" E) and
69 Funtana (45°10'39" N, 13°35'42" E), by diving (depth, ~1.5 m) in 10 l containers and transported
70 to the laboratory where 10 – 20 l were filtered through a 20 µm mesh net. The filtrate was further
71 sequentially filtered using a peristaltic pump through 3 µm and 0.2 µm polycarbonate membrane
72 filters (Whatman, United Kingdom). Filters were dried briefly at room temperature and stored at
73 –80 °C. Samples were collected monthly from July 2017 to October 2018. At the same time when
74 samples for picoplankton community structure assessment were collected additional samples were
75 retrieved to determined a set of environmental parameters as reported previously (Najdek et al.,
76 2020a, 2020b).

77 **DNA isolation**

78 Picoplankton DNA was isolated from 0.2 µm polycarbonate filters according to Massana et
79 al. (1997) with slight modifications. Following phenol-chloroform extractions, 1/10 of 3 M chilled
80 sodium acetate (pH 5.2) was added. DNA was precipitated by the addition of 1 volume of chilled
81 isopropanol, incubating the mixtures overnight at –20 °C and centrifuging at 20,000 × g and 4 °C
82 for 21 min. Pellets were washed twice with 500 µl of 70 % chilled ethanol and centrifuged after
83 each washing step at 20,000 × g and 4 °C for 5 min. Air-dried pellets were re-suspended in 50 µl of
84 deionized water.

85 **Illumina 16S rRNA sequencing**

86 The V4 region of the gene for 16S rRNA was sequenced using the Illumina MiSeq platform
87 as described previously (Korlević et al., submitted). A two-step PCR procedure was applied to
88 amplify the target region. In the first PCR, primers 515F (5'-GTGYCAGCMGCCGCGTAA-3')
89 and 806R (5'-GGACTACNVGGTWTCTAAT-3') from the Earth Microbiome Project (<https://earthmicrobiome.org/protocols-and-standards/16s/>) were used (Caporaso et al., 2012; Apprill
90 et al., 2015; Parada et al., 2016). A tagged sequence was added to these primers on their 5'
91 end. PCR products were purified and sent for Illumina MiSeq sequencing at IMGM Laboratories,
92 Martinsried, Germany. Prior to sequencing at IMGM, adapter and sample-specific index sequences
93 were incorporated during the second PCR amplification of the two-step PCR procedure using
94 primers targeting the tagged region. Beside samples, a positive and negative control were included
95 in each sequencing batch. For a positive control a mock community consisting of evenly mixed
96 DNA material originating from 20 bacterial strains (ATCC MSA-1002, ATCC, USA) was used,
97 while the negative control comprised PCR reactions without DNA template. Reads obtained in
98 this study (Bay of Saline) were combined with reads previously reported in a study describing
99 temporal dynamics of surface associated microbial communities (Bay of Funtana) (Korlević et al.,
100 submitted) and analysed together. Sequences processed in this study have been deposited in the
101 European Nucleotide Archive (ENA) at EMBL-EBI under accession numbers SAMEA6648771 –
102 SAMEA6648788, SAMEA6648824, SAMEA6648825, SAMEA8117500 – SAMEA8117516.

104 **Sequence analysis**

105 Sequences obtained in the present study were analysed using mothur (version 1.43.0) (Schloss
106 et al., 2009) according to the MiSeq Standard Operating Procedure (MiSeq SOP; https://mothur.org/wiki/MiSeq_SOP) (Kozich et al., 2013) and recommendations given by the Riffomonas project
107 to enhance data reproducibility (<http://www.riffomonas.org/>). Computing was performed on the
108

109 computer cluster Isabella (University Computing Center, University of Zagreb). Alignment and
110 classification was performed using the SILVA SSU Ref NR 99 database (release 138; [http://www.
arb-silva.de](http://www.arb-silva.de)) (Quast et al., 2013; Yilmaz et al., 2014). Pipeline data processing and visualisation
111 was done using R (version 3.6.0) (R Core Team, 2019) in combination with packages vegan (version
112 2.5.6) (Oksanen et al., 2019), tidyverse (version 1.2.1) (Wickham, 2017; Wickham et al., 2019)
113 and multiple other packages (Neuwirth, 2014; Xie, 2014, 2015, 2019a, 2019b, 2019c; Xie et al.,
114 2018; Allaire et al., 2019; McKinnon Edwards, 2019; Wilke, 2019; Zhu, 2019). The detailed
115 analysis procedure including the RMarkdown file are available in the GitHub repository (https://github.com/MicrobesRovinj/Korlevic_SeawaterDynamics_x_2021). The average sequencing error
116 rate of 0.01 % was calculated based on the ATCC MSA-1002 mock community included in each
117 sequencing batch, which is in line with previously reported values for next-generation 16S rRNA
118 amplicon sequencing (Kozich et al., 2013; Schloss et al., 2016). Also, negative controls processed
119 together with the samples yielded on average only 2 sequences after quality curation.

122 **Results**

123 Sequencing of 17 samples from the Bay of Saline and 18 samples from the Bay of Funtana
124 (one of the samples was a sequencing replicate) yielded 1.6 million reads after quality curation and
125 exclusion of sequences without known relatives (no relative sequences), eukaryotic, chloroplast and
126 mitochondrial sequences (Table S1). The number of reads per sample ranged from 25,360 to 77,466
127 (Fig. S1 and Table S1). Reads were clustered into 16,629 different OTUs at a similarity level of 97
128 %. To account for different sequencing depth reads were normalized to the minimum number of
129 sequences per sample (25,360, Table S1) that resulted in 13,440 different OTUs ranging from 608
130 to 1,790 OTUs per sample (Fig. S2).

131 Temporal variations in richness and diversity were determined by calculating the observed
132 number of OTUs, Chao1, ACE, Exponential Shannon and Inverse Simpson (Jost, 2006). Similar
133 trends in richness and diversity were observed at both stations (Fig. S2) characterized by a December
134 2017 richness maximum both in the Saline (Number of OTUs, 1,790 OTUs) and Funtana (Number
135 of OTUs, 1,786 OTUs) Bay. Interestingly, the Inverse Simpson index did not show an elevated
136 value in December 2017 as the Exponential Shannon index indicating that rare OTUs contributed
137 substantially to the observed richness maxima. To determine temporal changes in the proportion of
138 shared OTUs and communities the Jaccard's and Bray-Curtis similarity coefficients were calculated
139 between consecutive sampling points (Fig. S3). Similar trends were observed at both stations
140 with higher stability of shared bacterial and archaeal OTUs (Jaccard's similarity coefficient) than
141 shared communities (Bray-Curtis similarity coefficient). In addition, a stronger drop in shared
142 communities between March and April 2018 was observed at both stations indicating a more
143 pronounced community shift in this period (Fig. S3). Analysis of this time series data showed
144 that only 0.3 % of OTUs were present throughout the study period while these persistent OTUs
145 contributed to 62.0 % of sequences.

146 To evaluate the temporal variation of bacterial and archaeal communities Principal Coordinate

¹⁴⁷ Analysis (PCoA) of Bray-Curtis distances was applied to the OTU community data (Fig. 1A).
¹⁴⁸ Communities specific to summer, autumn/winter and spring could be identified regardless of
¹⁴⁹ the station sampled. This separation in three specific communities was further supported by
¹⁵⁰ ANOSIM ($R = 0.72$, $p < 0.01$). To assess which environmental parameter mainly contributes to the
¹⁵¹ observed temporal community variation the community data was constrained by a set of previously
¹⁵² reported environmental variables (Najdek et al., 2020a, 2020b) using Distance-Based Redundancy
¹⁵³ Analysis (db-RDA) (Fig. 1B). Nearly half ($R_a^2 = 45.5\%$) of the observed community variation
¹⁵⁴ could be explained by the explanatory variables. Separation between summer and autumn/winter
¹⁵⁵ communities could mainly be explained by temperature, prokaryotic abundance, salinity and nitrite.
¹⁵⁶ In contrast, neither variable could strongly explain the separate spring community.

¹⁵⁷ The classification of reads showed that the prokaryotic community was dominated by bacterial
¹⁵⁸ ($98.3 \pm 3.5\%$) over archaeal sequences ($1.7 \pm 3.5\%$) (Fig. 2). A higher relative contribution
¹⁵⁹ of archaeal reads was observed only in November 2017 ($7.5 \pm 2.2\%$), December 2017 ($13.2 \pm$
¹⁶⁰ 1.4%) and February 2018 ($3.7 \pm 0.9\%$). The main taxonomic group contributing to the higher
¹⁶¹ relative abundance of *Archaea* in this period was the *Crenarchaeota* “*Candidatus Nitrosopumilus*”
¹⁶² and the *Thermoplasmatota* Marine group II. The bacterial community was comprised of well
¹⁶³ known seawater groups such as the *Actinobacteriota*, *Bacteroidota*, *Cyanobacteria*, *Marinimicrobia*,
¹⁶⁴ *Alphaproteobacteria*, *Gammaproteobacteria* and *Verrucomicrobiota* (Fig. 2). In addition, similar
¹⁶⁵ temporal patterns were observed at both stations.

¹⁶⁶ *Cyanobacteria* comprised on average $5.1 \pm 2.8\%$ of the prokaryotic community. The
¹⁶⁷ highest relative contribution was recorded in winter ($8.2 \pm 5.6\%$), mainly caused by the high
¹⁶⁸ proportion in the March 2018 sample ($13.0 \pm 1.6\%$). The cyanobacterial community was largely
¹⁶⁹ dominated by *Synechococcus*, especially during periods of higher cyanobacterial presence (Fig. 3).
¹⁷⁰ *Bacteroidota* comprised on average $21.8 \pm 6.2\%$ of the community. Slightly higher values were
¹⁷¹ characteristic for spring and summer ($23.9 \pm 4.6\%$) in comparison to autumn and winter ($18.0 \pm$
¹⁷² 7.1%) (Fig. 2). Although *Bacteroidota* showed only slight temporal variations, taxa within

173 this group exhibited strong seasonal patterns (Fig. 4). Groups such as the NS5 marine group
174 and uncultured *Cryomorphaceae* were present throughout the year, while sequences classified as
175 *Balneola*, uncultured *Balneolaceae* and the NS11-12 marine group were more pronounced from
176 May to October. In addition, *Formosa* and the NS4 marine group could be detected throughout the
177 study period but specifically contributed to the *Bacteroidota* community in March and April 2018,
178 respectively. Higher values of chloroplast sequences were also recorded at this time (Fig. S4). In
179 addition, while uncultured *Saprospiraceae* from the Saline Bay samples contributed substantially to
180 the *Bacteroidota* community in June and July 2018, this phenomenon was not as pronounced in the
181 Funtana Bay (Fig. 4).

182 Sequences classified as *Alphaproteobacteria* showed the highest relative abundance and
183 comprised on average $38.3 \pm 8.0\%$ of the prokaryotic community (Fig. 2). Analysis of temporal
184 alphaproteobacterial variation showed higher sequence contribution in summer ($41.3 \pm 6.3\%$)
185 and winter ($44.0 \pm 2.2\%$) in comparison to autumn ($34.9 \pm 4.9\%$) and spring ($31.1 \pm 11.5\%$).
186 Temporal variation of taxa within this class showed different patterns (Fig. 5). The most pronounced
187 community shift was observed in April 2018 when reads of the usually prominent SAR11 clade
188 were scarce and *Stappiaceae*, *Ascidiaeihabitans* and no relative *Rhodobacteraceae* dominated
189 the alphaproteobacterial community. Subclades within the SAR11 clade also showed different
190 temporal patterns. Subclades II and III characterized the SAR11 community in summer from June
191 to September, while from November to March reads classified as subclade Ia comprised the majority
192 of SAR11 specific sequences. Except by the SAR11 subclades II and III, summer months were also
193 characterized by two other alphaproteobacterial groups, the HIMB11 and the AEGEAN-169 marine
194 group (Fig. 5).

195 Reads classified as *Gammaproteobacteria* comprised on average $21.6 \pm 6.6\%$ of the
196 prokaryotic community (Fig. 2). The season characterized by the highest relative contribution of
197 gammaproteobacterial sequences was spring ($29.9 \pm 12.3\%$), while in other periods values ranged
198 from 18.9 ± 2.6 to $22.3 \pm 2.5\%$. Temporal variation analysis of taxa within *Gammaproteobacteria*

199 showed groups present throughout the year, such as the SAR86 clade, but also season specific taxa,
200 such as *Litoricola*, OM60 (NOR5) clade and SUP05 cluster (Fig. 6). *Litoricola* and the OM60
201 (NOR5) clade characterized the gammaproteobacterial community from April to August, while
202 sequences specific for the SUP05 cluster were detected from November to March. Taxonomic
203 groups of high level bacterial taxa that comprised a lower proportion of prokaryotic sequences
204 such as the *Actinobacteriota* and *Verrucomicrobiota* also showed temporal variations. During
205 the period of higher relative sequence abundance of *Actinobacteriota*, in the time span between
206 September and December, the actinobacterial community was comprised mainly of the “*Candidatus*
207 *Actinomarina*”. Similarly, in April and May when *Verrucomicrobiota* specific reads were at their
208 maximal relative abundance *Lentimonas* and *Coraliomargarita* were the main constituent of the
209 *Verrucomicrobiota* specific community.

210 **Discussion**

211 Prokaryotic communities inhabiting surface waters of temporal areas exhibit patterns of
212 seasonal succession (Bunse and Pinhassi, 2017). These temporal variations were mainly studied at
213 long-term time series sites which usually encompass only one sampling station located further away
214 from the coast (Gilbert et al., 2009; Mestre et al., 2020). In the present study temporal variation
215 of surface prokaryotic communities was determined in the close proximity of the shore. Drawn
216 conclusions were further strengthen by the analysis of time series data at two closely located stations.
217 Similar patterns were observed at both sites indicating that determined phenomena could also be
218 characteristic for prokaryotic communities inhabiting surface waters of a wider area.

219 Temporal changes in richness were substantial as indicated by the proportion of OTUs present
220 at every sampling point (0.3 %). Sequences clustered into these persistent OTUs comprised a high
221 proportion of reads (62.0 %). Similar proportions of persistent core OTUs and their contribution
222 to the total number of sequences were also reported in other time series studies (Gilbert et al.,
223 2009, 2012). Analysis of temporal variations in alpha diversity showed maximal richness values in
224 December. This observed event is in line with previously reported richness maxima in other areas
225 during colder months (Gilbert et al., 2012; Ladau et al., 2013; El-Swais et al., 2015; Mestre et al.,
226 2020). It has been suggested that late autumn/winter overturn is responsible for this phenomenon
227 by simply mixing population from deeper parts of the water column with existing ones (García et
228 al., 2015; Salter et al., 2015; Bunse and Pinhassi, 2017). Although the samples in this study were
229 retrieved at very shallow locations, water column mixing taking place at deeper areas could bring
230 additional taxa to these locations causing the observed increase in alpha diversity.

231 The majority of studies analysing temporal community variation usually identified an exchange
232 of multiple community states during the year (El-Swais et al., 2015; Lindh et al., 2015). In contrast,
233 some studies described only a switch between winter and summer specific assemblages (Ward et al.,
234 2017; Mestre et al., 2020). It is possible that these differences are a consequence of local conditions.

Indeed, some studies attributed the observed lower number of states to the absence of large spring and fall phytoplankton blooms in some areas (Ward et al., 2017). Analysis of OTU community data from our samples identified three separate microbial assemblages characteristic for spring, summer and autumn/winter. This is in line with studies describing the exchange of multiple states during the year with a separate spring community assemblage (El-Swais et al., 2015; Lindh et al., 2015). We hypothesize that the separate spring community is a late response to a phytoplankton bloom that can occur in this area (Mozetič et al., 2010; Manna et al., 2021). Temperature and prokaryotic abundance were identified as the main factors influencing the exchange of communities between the summer and autumn/winter period. It is not surprising that temperature and prokaryotic abundance are similar in explaining this shift as higher prokaryotic abundances were reported in this area during summer months (Ivančić et al., 2010). The identification of temperature as the single most important driver of community change is in line with previously reported data (El-Swais et al., 2015; Ward et al., 2017; Mestre et al., 2020). It was proposed that temperature indirectly influences community change through phytoplankton nutrient limitation during water column stratification and nutrient input in times of water column mixing (Bunse and Pinhassi, 2017). Factors explaining the onset of a separate spring community were not identified. We hypothesize that based on a slightly higher value of chloroplast specific reads in these samples and the presence of taxa specific for phytoplankton blooms this community was a late prokaryotic response to a phytoplankton bloom even though the concentration of chlorophyll *a* could not explain it.

Differences between communities specific for spring, summer and autumn/winter observed at the level of OTUs could also be seen in the taxonomic composition. The identified spring-specific community contained taxa previously associated with phytoplankton blooms (Teeling et al., 2012, 2016; Sintes et al., 2013). *Formosa* and members within the *Rhodobacteraceae* were associated with phytoplankton blooms in the North Sea (Teeling et al., 2012, 2016), while the NS4 marine group was found in previous studies describing bacterial communities in different environments of the Adriatic Sea with no clear association with increased autotrophic biomass (Korlević et al., 2015, 2016). Observed variations in spring communities between different areas could be

262 explained by differences in structure and supply of phototroph-derived organic matter. The
263 summer community was characterized by the family *Balneolaceae* and the NS11-12 marine group
264 from the *Bacteroidota*, the SAR11 subclades II and III, HIMB11 and the AEGEAN-169 marine
265 group from the *Alphaproteobacteria* and from the *Gammaproteobacteria* the OM60 (NOR5)
266 clade and *Litoricola*. In contrast, the winter community was characterized by the archaeal
267 “*Candidatus Nitrosopumilus*” and Marine group II, the alphaproteobacterial SAR11 subclade Ia
268 and the gammaproteobacterial SUP05 cluster. Temporal and depth-related variation of different
269 SAR11 subclades was also reported previously although in our data a different pattern could be
270 observed in comparison to other surface associated SAR11 communities (Carlson et al., 2009;
271 Vergin et al., 2013; Salter et al., 2015). In example, the higher contribution of the SAR11 subclade
272 Ia to the community in winter. Higher contribution of members in the summer community such as
273 the HIMB11, the OM60 (NOR5) clade and *Litoricola* could result from their adaptation to more
274 oligotrophic conditions during water column stratification in summer through the ability to use
275 alternative methods of energy supply (i.e. bacteriochlorophyll *a* and proteorhodopsin) (Huggett and
276 Rappe, 2012; Spring and Riedel, 2013; Durham et al., 2014). Furthermore, higher contribution of
277 the AEGEAN-169 marine group to the summer community in our samples could be explained by
278 the hypothesised adaptation of this group to ultraoligotrophic waters and high solar irradiance
279 (Reintjes et al., 2019). The co-occurrence of “*Candidatus Nitrosopumilus*” and the Marine
280 group II in winter samples is interesting. A study describing a strong co-dominance of these two
281 groups suggested that nitrification by ammonia-oxidising archaea is coupled with ammonification
282 performed by the members of the Marine group II (Kim et al., 2019). In addition, the presence of
283 “*Candidatus Nitrosopumilus*” reads in our samples is not surprising as recently two new strains
284 of ammonia-oxidising archaea within the genus *Nitrosopumilus* have been isolated from northern
285 Adriatic coastal waters (Bayer et al., 2019).

286 Beside these groups that showed specificity to one of the identified temporal communities
287 taxonomic analysis revealed taxa present through the year, such as the cyanobacterial *Synechococcus*,
288 the flavobacterial NS5 marine group and *Cryomorphaceae* and the gammaproteobacterial SAR86

289 clade. The dominance of *Synechococcus* over other cyanobacterial groups in this coastal area was
290 reported previously, so it is not surprising that we also observed a strong dominance of *Synechococcus*
291 related sequences (Šilović et al., 2012; Tinta et al., 2015). The known genome versatility of
292 *Synechococcus* could explain the high contribution of this genus to the cyanobacterial community in
293 fluctuating coastal environments (Palenik et al., 2003). The *Cryomorphaceae* were associated with
294 organic matter remineralisation processes (Bowman, 2014), while a single-cell genome analysis
295 of the NS5 marine group revealed the ability to degrade marine polysaccharides. In addition, the
296 NS5 marine group was previously detected in different seasons and environments of the Adriatic
297 Sea (Korlević et al., 2015, 2016). It seems that members of these two groups are part of a basic
298 remineralisation community present at this location throughout the year. The gammaproteobacterial
299 SAR86 clade, previously reported in different environments of the Adriatic Sea (Korlević et al., 2015,
300 2016; Tinta et al., 2015), was also detected throughout the year. Recent analysis of metagenomic
301 data suggested the existence of different functional and ecological ecotypes of this ubiquitous clade
302 (Hoarfrost et al., 2020). It is possible that different ecotypes are also characteristic for different
303 seasons.

304 In conclusion, prokaryotic communities inhabiting the proximity of the shore exhibit temporal
305 variations similar to surface water assemblages in other temperate areas. As in other areas a richness
306 maximum was recorded in the colder period of the year, the exchange of multiple community states
307 during the year was observed and temperature was identified as the main force driving temporal
308 community change (Gilbert et al., 2012; Ladau et al., 2013; El-Swais et al., 2015; Lindh et al., 2015;
309 Ward et al., 2017; Mestre et al., 2020). Beside these similarities, temporal analysis of taxonomic data
310 identified season-specific community structures and groups exhibiting temporal patterns different
311 from other areas indicating that beside global driving factors local conditions also influence the
312 coastal prokaryotic community.

313 **Acknowledgments**

314 This study was funded by the Croatian Science Foundation through the MICRO-SEAGRASS
315 project (project number IP-2016-06-7118). GJH was supported by the Austrian Science Fund
316 (FWF) through the ARTEMIS project (project number P28781-B21). We would like to thank the
317 University Computing Center of the University of Zagreb for access to the computer cluster Isabella,
318 Margareta Buterer for technical support and Paolo Paliaga for help during sampling.

319 **References**

- 320 Allaire, J. J., Xie, Y., McPherson, J., Luraschi, J., Ushey, K., Atkins, A., et al. (2019).
- 321 *rmarkdown: Dynamic documents for R.*
- 322 Alonso-Sáez, L., Balagué, V., Sà, E. L., Sánchez, O., González, J. M., Pinhassi, J., et
323 al. (2007). Seasonality in bacterial diversity in north-west Mediterranean coastal waters:
324 Assessment through clone libraries, fingerprinting and FISH. *FEMS Microbiol. Ecol.* 60, 98–112.
325 doi:10.1111/j.1574-6941.2006.00276.x.
- 326 Alonso-Sáez, L., Díaz-Pérez, L., and Morán, X. A. G. (2015). The hidden seasonality of
327 the rare biosphere in coastal marine bacterioplankton. *Environ. Microbiol.* 17, 3766–3780.
328 doi:10.1111/1462-2920.12801.
- 329 Apprill, A., McNally, S., Parsons, R., and Weber, L. (2015). Minor revision to V4 region SSU
330 rRNA 806R gene primer greatly increases detection of SAR11 bacterioplankton. *Aquat. Microb.
331 Ecol.* 75, 129–137. doi:10.3354/ame01753.
- 332 Bayer, B., Vojvoda, J., Reinthaler, T., Reyes, C., Pinto, M., and Herndl, G. J. (2019).
333 *Nitrosopumilus adriaticus* sp. nov. and *Nitrosopumilus piranensis* sp. nov., two ammonia-oxidizing
334 archaea from the Adriatic Sea and members of the class *Nitrososphaeria*. *Int J Syst Evol Microbiol*
335 69, 1892–1902. doi:10.1099/ijsem.0.003360.
- 336 Bowman, J. P. (2014). “The family *Cryomorphaceae*,” in *The Prokaryotes: Other
337 Major Lineages of Bacteria and the Archaea*, eds. E. Rosenberg, E. F. DeLong, S. Lory,
338 E. Stackebrandt, and F. Thompson (Berlin, Heidelberg: Springer-Verlag), 539–550.
339 doi:10.1007/978-3-642-38954-2_135.
- 340 Bunse, C., and Pinhassi, J. (2017). Marine bacterioplankton seasonal succession dynamics.
341 *Trends in Microbiology* 25, 494–505. doi:10.1016/j.tim.2016.12.013.

- 342 Caporaso, J. G., Lauber, C. L., Walters, W. A., Berg-Lyons, D., Huntley, J., Fierer, N., et al.
343 (2012). Ultra-high-throughput microbial community analysis on the Illumina HiSeq and MiSeq
344 platforms. *ISME J.* 6, 1621–1624. doi:10.1038/ismej.2012.8.
- 345 Carlson, C. A., Morris, R., Parsons, R., Treusch, A. H., Giovannoni, S. J., and Vergin, K.
346 (2009). Seasonal dynamics of SAR11 populations in the euphotic and mesopelagic zones of the
347 northwestern Sargasso Sea. *ISME J.* 3, 283–295. doi:10.1038/ismej.2008.117.
- 348 Durham, B. P., Grote, J., Whittaker, K. A., Bender, S. J., Luo, H., Grim, S. L., et al.
349 (2014). Draft genome sequence of marine alphaproteobacterial strain HIMB11, the first cultivated
350 representative of a unique lineage within the *Roseobacter* clade possessing an unusually small
351 genome. *Stand Genomic Sci* 9, 632–645. doi:10.4056/sigs.4998989.
- 352 El-Swais, H., Dunn, K. A., Bielawski, J. P., Li, W. K. W., and Walsh, D. A. (2015). Seasonal
353 assemblages and short-lived blooms in coastal north-west Atlantic Ocean bacterioplankton. *Environ.*
354 *Microbiol.* 17, 3642–3661. doi:10.1111/1462-2920.12629.
- 355 Fuhrman, J. A., Cram, J. A., and Needham, D. M. (2015). Marine microbial
356 community dynamics and their ecological interpretation. *Nat. Rev. Microbiol.* 13, 133–146.
357 doi:10.1038/nrmicro3417.
- 358 García, F. C., Alonso-Sáez, L., Morán, X. A. G., and López-Urrutia, Á. (2015). Seasonality in
359 molecular and cytometric diversity of marine bacterioplankton: The re-shuffling of bacterial taxa by
360 vertical mixing. *Environ. Microbiol.* 17, 4133–4142. doi:10.1111/1462-2920.12984.
- 361 Gilbert, J. A., Field, D., Swift, P., Newbold, L., Oliver, A., Smyth, T., et al. (2009). The
362 seasonal structure of microbial communities in the Western English Channel. *Environ. Microbiol.*
363 11, 3132–3139. doi:10.1111/j.1462-2920.2009.02017.x.

³⁶⁴ Gilbert, J. A., Steele, J. A., Caporaso, J. G., Steinbrück, L., Reeder, J., Temperton, B., et
³⁶⁵ al. (2012). Defining seasonal marine microbial community dynamics. *ISME J.* 6, 298–308.
³⁶⁶ doi:10.1038/ismej.2011.107.

³⁶⁷ Hoarfrost, A., Nayfach, S., Ladau, J., Yooseph, S., Arnosti, C., Dupont, C. L., et al.
³⁶⁸ (2020). Global ecotypes in the ubiquitous marine clade SAR86. *ISME J.* 14, 178–188.
³⁶⁹ doi:10.1038/s41396-019-0516-7.

³⁷⁰ Huggett, M. J., and Rappe, M. S. (2012). Genome sequence of strain HIMB30, a novel member
³⁷¹ of the marine *Gammaproteobacteria*. *J. Bacteriol.* 194, 732–733. doi:10.1128/JB.06506-11.

³⁷² Ivančić, I., Fuks, D., Najdek, M., Blažina, M., Devescovi, M., Šilović, T., et al. (2010).
³⁷³ Long-term changes in heterotrophic prokaryotes abundance and growth characteristics in the
³⁷⁴ northern Adriatic Sea. *J. Mar. Syst.* 82, 206–216. doi:10.1016/J.JMARSYS.2010.05.008.

³⁷⁵ Jost, L. (2006). Entropy and diversity. *Oikos* 113, 363–375.
³⁷⁶ doi:10.1111/j.2006.0030-1299.14714.x.

³⁷⁷ Kim, J.-G., Gwak, J.-H., Jung, M.-Y., An, S.-U., Hyun, J.-H., Kang, S., et al. (2019). Distinct
³⁷⁸ temporal dynamics of planktonic archaeal and bacterial assemblages in the bays of the Yellow Sea.
³⁷⁹ *PloS one* 14, e0221408. doi:10.1371/journal.pone.0221408.

³⁸⁰ Korlević, M., Markovski, M., Zhao, Z., Herndl, G. J., and Najdek, M. Seasonal dynamics of
³⁸¹ epiphytic microbial communities on marine macrophyte surfaces.

³⁸² Korlević, M., Markovski, M., Zhao, Z., Herndl, G. J., and Najdek, M. Selective DNA and
³⁸³ protein isolation from marine macrophyte surfaces.

³⁸⁴ Korlević, M., Pop Ristova, P., Garić, R., Amann, R., and Orlić, S. (2015). Bacterial diversity
³⁸⁵ in the South Adriatic Sea during a strong, deep winter convection year. *Appl. Environ. Microbiol.*
³⁸⁶ 81, 1715–1726. doi:10.1128/AEM.03410-14.

- 387 Korlević, M., Šupraha, L., Ljubešić, Z., Henderiks, J., Ciglenečki, I., Dautović, J., et al. (2016).
- 388 Bacterial diversity across a highly stratified ecosystem: A salt-wedge Mediterranean estuary. *Syst.*
- 389 *Appl. Microbiol.* 39, 398–408. doi:10.1016/j.syapm.2016.06.006.
- 390 Kozich, J. J., Westcott, S. L., Baxter, N. T., Highlander, S. K., and Schloss, P. D. (2013).
- 391 Development of a dual-index sequencing strategy and curation pipeline for analyzing amplicon
- 392 sequence data on the MiSeq Illumina sequencing platform. *Appl. Environ. Microbiol.* 79,
- 393 5112–5120. doi:10.1128/AEM.01043-13.
- 394 Ladau, J., Sharpton, T. J., Finucane, M. M., Jospin, G., Kembel, S. W., O'Dwyer, J., et al.
- 395 (2013). Global marine bacterial diversity peaks at high latitudes in winter. *ISME J.* 7, 1669–1677.
- 396 doi:10.1038/ismej.2013.37.
- 397 Lindh, M. V., Sjöstedt, J., Andersson, A. F., Baltar, F., Hugerth, L. W., Lundin, D., et al. (2015).
- 398 Disentangling seasonal bacterioplankton population dynamics by high-frequency sampling. *Environ.*
- 399 *Microbiol.* 17, 2459–2476. doi:10.1111/1462-2920.12720.
- 400 Manna, V., De Vittor, C., Giani, M., Del Negro, P., and Celussi, M. (2021). Long-term patterns
- 401 and drivers of microbial organic matter utilization in the northernmost basin of the Mediterranean
- 402 Sea. *Mar. Environ. Res.* 164, 105245. doi:10.1016/j.marenvres.2020.105245.
- 403 Massana, R., Murray, A. E., Preston, C. M., and DeLong, E. F. (1997). Vertical distribution
- 404 and phylogenetic characterization of marine planktonic *Archaea* in the Santa Barbara Channel. *Appl.*
- 405 *Environ. Microbiol.* 63, 50–56.
- 406 McKinnon Edwards, S. (2019). *lemon: Freshing up your 'ggplot2' plots.*
- 407 Mestre, M., Höfer, J., Sala, M. M., and Gasol, J. M. (2020). Seasonal variation of
- 408 bacterial diversity along the marine particulate matter continuum. *Front. Microbiol.* 11, 1590.
- 409 doi:10.3389/fmicb.2020.01590.

410 Mozetič, P., Solidoro, C., Cossarini, G., Socal, G., Precali, R., Francé, J., et al. (2010). Recent
411 trends towards oligotrophication of the Northern Adriatic: Evidence from chlorophyll *a* time series.
412 *Estuaries Coast* 33, 362–375. doi:10.1007/s12237-009-9191-7.

413 Najdek, M., Korlević, M., Paliaga, P., Markovski, M., Ivančić, I., Iveša, L., et al. (2020a).
414 Dynamics of environmental conditions during the decline of a *Cymodocea nodosa* meadow.
415 *Biogeosciences* 17, 3299–3315. doi:10.5194/bg-17-3299-2020.

416 Najdek, M., Korlević, M., Paliaga, P., Markovski, M., Ivančić, I., Iveša, L., et al. (2020b).
417 Effects of the invasion of *Caulerpa cylindracea* in a *Cymodocea nodosa* meadow in the Northern
418 Adriatic Sea. *Front. Mar. Sci.* 7, 602055. doi:10.3389/fmars.2020.602055.

419 Needham, D. M., and Fuhrman, J. A. (2016). Pronounced daily succession of
420 phytoplankton, archaea and bacteria following a spring bloom. *Nat. Microbiol.* 1, 1–7.
421 doi:10.1038/nmicrobiol.2016.5.

422 Neuwirth, E. (2014). *RColorBrewer: ColorBrewer palettes*.

423 Oksanen, J., Blanchet, F. G., Friendly, M., Kindt, R., Legendre, P., McGlinn, D., et al. (2019).
424 *vegan: Community ecology package*.

425 Palenik, B., Brahamsha, B., Larimer, F. W., Land, M., Hauser, L., Chain, P., et al. (2003). The
426 genome of a motile marine *Synechococcus*. *Nature* 424, 1037–1042. doi:10.1038/nature01943.

427 Parada, A. E., Needham, D. M., and Fuhrman, J. A. (2016). Every base matters: Assessing
428 small subunit rRNA primers for marine microbiomes with mock communities, time series and
429 global field samples. *Environ. Microbiol.* 18, 1403–1414. doi:10.1111/1462-2920.13023.

430 Quast, C., Pruesse, E., Yilmaz, P., Gerken, J., Schweer, T., Yarza, P., et al. (2013). The SILVA
431 ribosomal RNA gene database project: Improved data processing and web-based tools. *Nucleic
432 Acids Res.* 41, D590–D596. doi:10.1093/nar/gks1219.

- 433 R Core Team (2019). *R: A language and environment for statistical computing*. Vienna,
434 Austria: R Foundation for Statistical Computing.
- 435 Reintjes, G., Tegetmeyer, H. E., Bürgisser, M., Orlić, S., Tews, I., Zubkov, M., et al. (2019).
436 On-site analysis of bacterial communities of the ultraoligotrophic South Pacific Gyre. *Appl. Environ.*
437 *Microbiol.* 85, e00184–19. doi:10.1128/AEM.00184-19.
- 438 Salter, I., Galand, P. E., Fagervold, S. K., Lebaron, P., Obernosterer, I., Oliver, M. J., et al.
439 (2015). Seasonal dynamics of active SAR11 ecotypes in the oligotrophic Northwest Mediterranean
440 Sea. *ISME J.* 9, 347–360. doi:10.1038/ismej.2014.129.
- 441 Schloss, P. D., Jenior, M. L., Koumpouras, C. C., Westcott, S. L., and Highlander, S. K. (2016).
442 Sequencing 16S rRNA gene fragments using the PacBio SMRT DNA sequencing system. *PeerJ* 4,
443 e1869. doi:10.7717/peerj.1869.
- 444 Schloss, P. D., Westcott, S. L., Ryabin, T., Hall, J. R., Hartmann, M., Hollister, E. B., et al.
445 (2009). Introducing mothur: Open-source, platform-independent, community-supported software
446 for describing and comparing microbial communities. *Appl. Environ. Microbiol.* 75, 7537–7541.
447 doi:10.1128/AEM.01541-09.
- 448 Sintes, E., Witte, H., Stodderegger, K., Steiner, P., and Herndl, G. J. (2013). Temporal dynamics
449 in the free-living bacterial community composition in the coastal North Sea. *FEMS Microbiol. Ecol.*
450 83, 413–424. doi:10.1111/1574-6941.12003.
- 451 Spring, S., and Riedel, T. (2013). Mixotrophic growth of bacteriochlorophyll *a*-containing
452 members of the OM60/NOR5 clade of marine gammaproteobacteria is carbon-starvation
453 independent and correlates with the type of carbon source and oxygen availability. *BMC Microbiol*
454 13, 117. doi:10.1186/1471-2180-13-117.

455 Šilović, T., Balagué, V., Orlić, S., and Pedrós-Alió, C. (2012). Picoplankton seasonal variation
456 and community structure in the northeast Adriatic coastal zone. *FEMS Microbiol. Ecol.* 82,
457 678–691. doi:10.1111/j.1574-6941.2012.01438.x.

458 Teeling, H., Fuchs, B. M., Becher, D., Klockow, C., Gardebrecht, A., Bennke, C. M., et
459 al. (2012). Substrate-controlled succession of marine bacterioplankton populations induced by a
460 phytoplankton bloom. *Science* 336, 608–611. doi:10.1126/science.1218344.

461 Teeling, H., Fuchs, B. M., Bennke, C. M., Krüger, K., Chafee, M., Kappelmann, L., et al.
462 (2016). Recurring patterns in bacterioplankton dynamics during coastal spring algae blooms. *eLife*
463 5, e11888. doi:10.7554/eLife.11888.

464 Tinta, T., Vojvoda, J., Mozetič, P., Talaber, I., Vodopivec, M., Malfatti, F., et al. (2015).
465 Bacterial community shift is induced by dynamic environmental parameters in a changing coastal
466 ecosystem (northern Adriatic, northeastern Mediterranean Sea) - a 2-year time-series study. *Environ.*
467 *Microbiol.* 17, 3581–3596. doi:10.1111/1462-2920.12519.

468 Vergin, K. L., Beszteri, B., Monier, A., Cameron Thrash, J., Temperton, B., Treusch, A. H., et al.
469 (2013). High-resolution SAR11 ecotype dynamics at the Bermuda Atlantic Time-series Study site
470 by phylogenetic placement of pyrosequences. *ISME J.* 7, 1322–1332. doi:10.1038/ismej.2013.32.

471 Ward, C. S., Yung, C.-M., Davis, K. M., Blinebry, S. K., Williams, T. C., Johnson, Z. I., et
472 al. (2017). Annual community patterns are driven by seasonal switching between closely related
473 marine bacteria. *ISME J.* 11, 1412–1422. doi:10.1038/ismej.2017.4.

474 Wickham, H. (2017). *tidyverse: Easily install and load the 'tidyverse'*.

475 Wickham, H., Averick, M., Bryan, J., Chang, W., McGowan, L. D., François, R., et al. (2019).
476 Welcome to the tidyverse. *J. Open Source Softw.* 4, 1686. doi:10.21105/joss.01686.

477 Wilke, C. O. (2019). *cowplot: Streamlined plot theme and plot annotations for 'ggplot2'*.

- 478 Xie, Y. (2014). "knitr: A comprehensive tool for reproducible research in R," in *Implementing*
479 *Reproducible Computational Research*, eds. V. Stodden, F. Leisch, and R. D. Peng (New York:
480 Chapman and Hall/CRC), 3–32.
- 481 Xie, Y. (2015). *Dynamic Documents with R and knitr*. 2nd ed. Boca Raton, Florida: Chapman
482 and Hall/CRC.
- 483 Xie, Y. (2019a). *knitr: A general-purpose package for dynamic report generation in R*.
- 484 Xie, Y. (2019b). TinyTeX: A lightweight, cross-platform, and easy-to-maintain LaTeX
485 distribution based on TeX Live. *TUGboat* 40, 30–32.
- 486 Xie, Y. (2019c). *tinytex: Helper functions to install and maintain 'TeX Live', and compile*
487 *'LaTeX' documents*.
- 488 Xie, Y., Allaire, J. J., and Grolemund, G. (2018). *R Markdown: The Definitive Guide*. 1st ed.
489 Boca Raton, Florida: Chapman and Hall/CRC.
- 490 Yilmaz, P., Parfrey, L. W., Yarza, P., Gerken, J., Pruesse, E., Quast, C., et al. (2014). The
491 SILVA and "All-Species Living Tree Project (LTP)" taxonomic frameworks. *Nucleic Acids Res.* 42,
492 D643–D648. doi:10.1093/nar/gkt1209.
- 493 Zhu, H. (2019). *kableExtra: Construct complex table with 'kable' and pipe syntax*.

494 **Figure legends**

495 **Fig. 1.** (A) Principal Coordinates Analysis (PCoA) of Bray-Curtis distances based on OTU
496 abundances of bacterial and archaeal communities sampled in Saline and Funtana Bay. The
497 proportion of explained variation by each axis is shown on the corresponding axis in parentheses.
498 (B) Distance-Based Redundancy Analysis (db-RDA) of Bray-Curtis distances based on the same
499 community data sampled at the same locations and constrained by a set of environmental parameters
500 (T – temperature, S – salinity, PO_4^{3-} – orthophosphate, NH_4^+ – ammonium, NO_2^- – nitrite, NO_3^- –
501 nitrate, SiO_4^{4-} – orthosilicate, PM – particulate matter, Chl *a* – chlorophyll *a* and PA – prokaryotic
502 abundance). Scaling type 1 was selected for the biplot. The proportion of community data variation
503 explained by environmental variables (R_a^2) is stated on the biplot, while the proportion of community
504 data variation explained by each canonical axis is shown on the corresponding axis in parentheses.
505 Samples in both plots originating from the same station or same season are labeled in different
506 shape and color.

507 **Fig. 2.** Taxonomic classification and relative contribution of the most abundant ($\geq 1\%$) bacterial and
508 archaeal sequences in communities sampled in Saline and Funtana Bay. No Relative – sequences
509 without known relatives

510 **Fig. 3.** Taxonomic classification and relative contribution of the most abundant ($\geq 1\%$)
511 cyanobacterial sequences in communities sampled in Saline and Funtana Bay. The proportion
512 of cyanobacterial sequences in the total bacterial and archaeal community is given above the
513 corresponding bar.

514 **Fig. 4.** Taxonomic classification and relative contribution of the most abundant ($\geq 1\%$) sequences
515 within the *Bacteroidota* in communities sampled in Saline and Funtana Bay. The proportion of
516 sequences classified as *Bacteroidota* in the total bacterial and archaeal community is given above the
517 corresponding bar. NR – No Relative (sequences without known relatives within the corresponding
518 group)

519 **Fig. 5.** Taxonomic classification and relative contribution of the most abundant ($\geq 2\%$)
520 alphaproteobacterial sequences in communities sampled in Saline and Funtana Bay. The proportion
521 of alphaproteobacterial sequences in the total bacterial and archaeal community is given above the
522 corresponding bar. NR – No Relative (sequences without known relatives within the corresponding
523 group)

524 **Fig. 6.** Taxonomic classification and relative contribution of the most abundant ($\geq 1\%$)
525 gammaproteobacterial sequences in communities sampled in Saline and Funtana Bay. The
526 proportion of gammaproteobacterial sequences in the total bacterial and archaeal community is
527 given above the corresponding bar. NR – No Relative (sequences without known relatives within
528 the corresponding group)

529 **Figures**

27

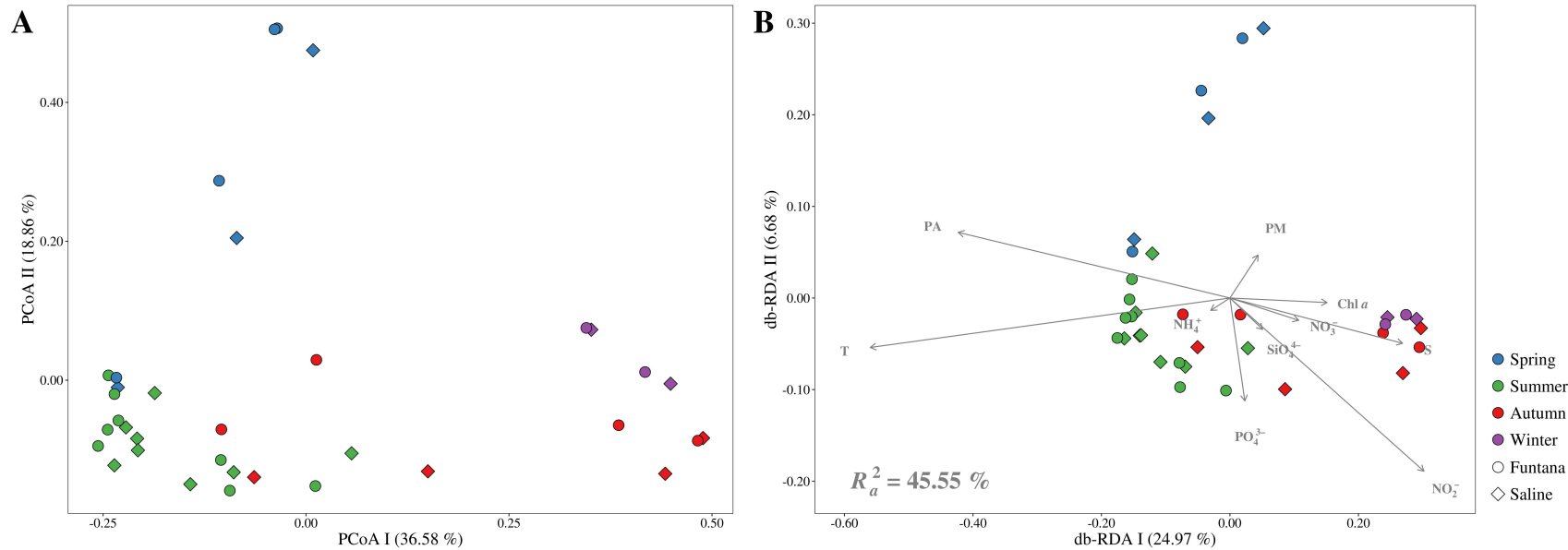


Fig. 1. (A) Principal Coordinates Analysis (PCoA) of Bray-Curtis distances based on OTU abundances of bacterial and archaeal communities sampled in Saline and Funtana Bay. The proportion of explained variation by each axis is shown on the corresponding axis in parentheses. (B) Distance-Based Redundancy Analysis (db-RDA) of Bray-Curtis distances based on the same community data sampled at the same locations and constrained by a set of environmental parameters (T – temperature, S – salinity, PO_4^{3-} – orthophosphate, NH_4^+ – ammonium, NO_2^- – nitrite, NO_3^- – nitrate, SiO_4^{4-} – orthosilicate, PM – particulate matter, Chl *a* – chlorophyll *a* and PA – prokaryotic abundance). Scaling type 1 was selected for the biplot. The proportion of community data variation explained by environmental variables (R_a^2) is stated on the biplot, while the proportion of community data variation explained by each canonical axis is shown on the corresponding axis in parentheses. Samples in both plots originating from the same station or same season are labeled in different shape and color.

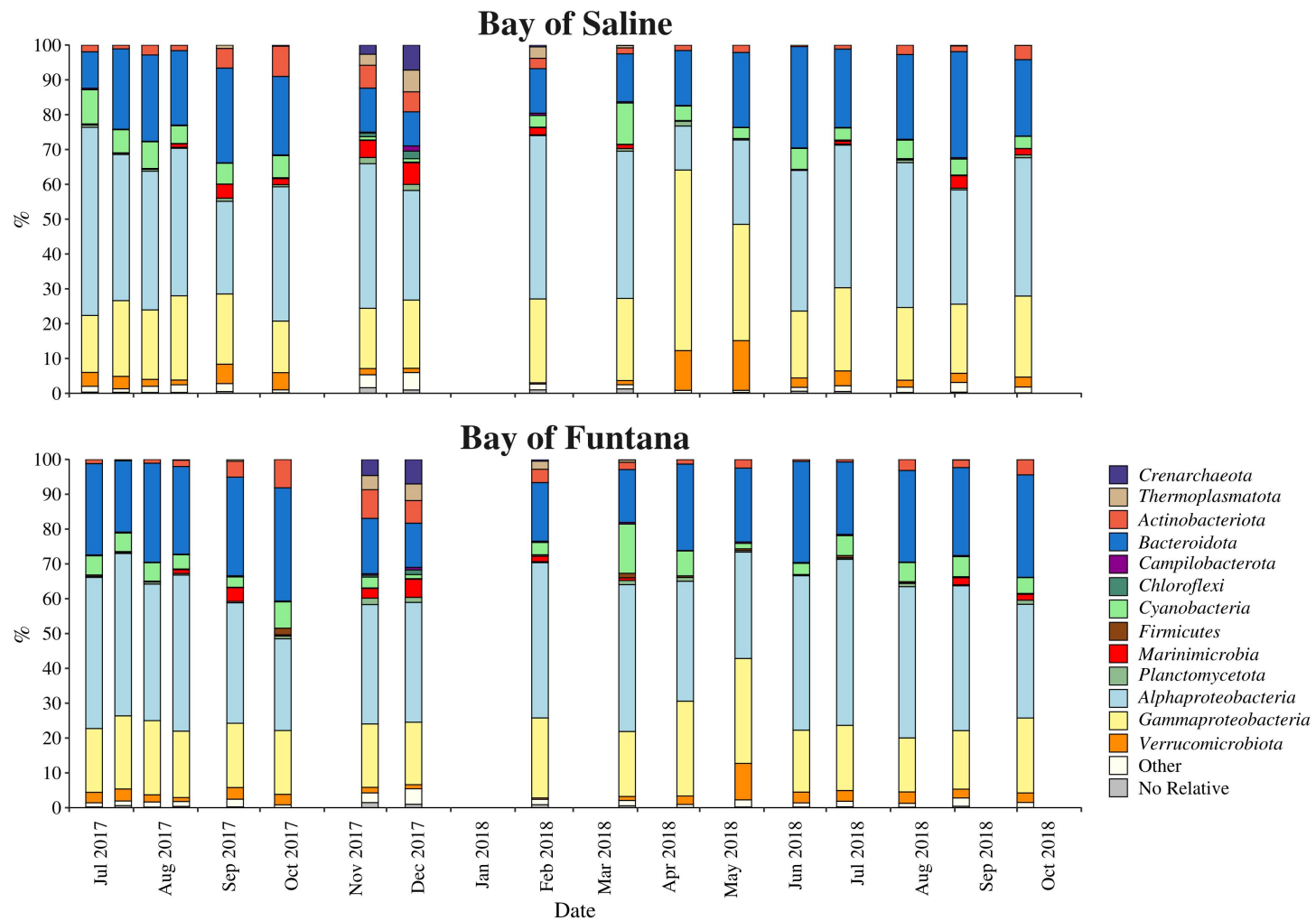


Fig. 2. Taxonomic classification and relative contribution of the most abundant ($\geq 1\%$) bacterial and archaeal sequences in communities sampled in Saline and Funtana Bay. No Relative – sequences without known relatives

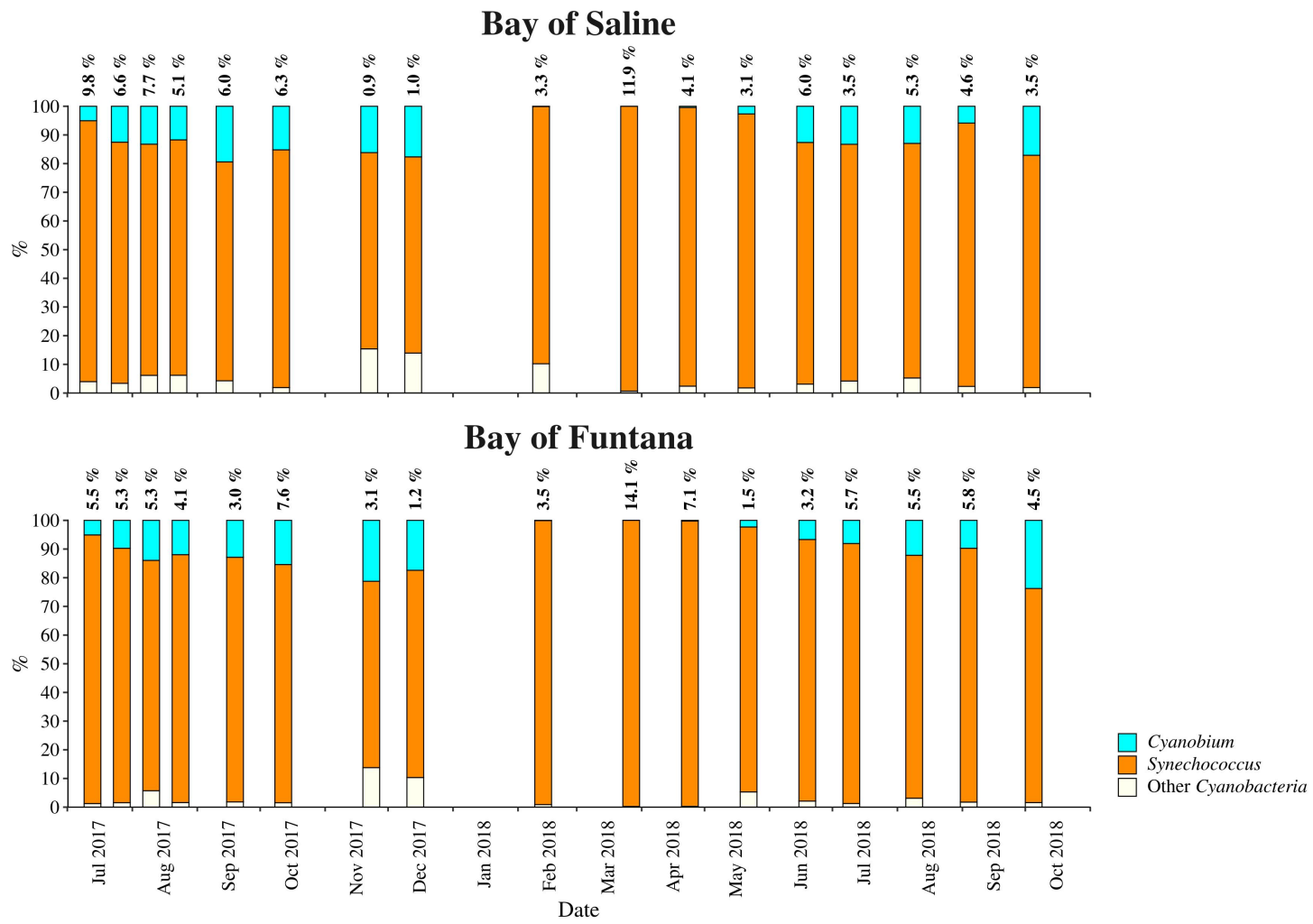


Fig. 3. Taxonomic classification and relative contribution of the most abundant ($\geq 1\%$) cyanobacterial sequences in communities sampled in Saline and Funtana Bay. The proportion of cyanobacterial sequences in the total bacterial and archaeal community is given above the corresponding bar.

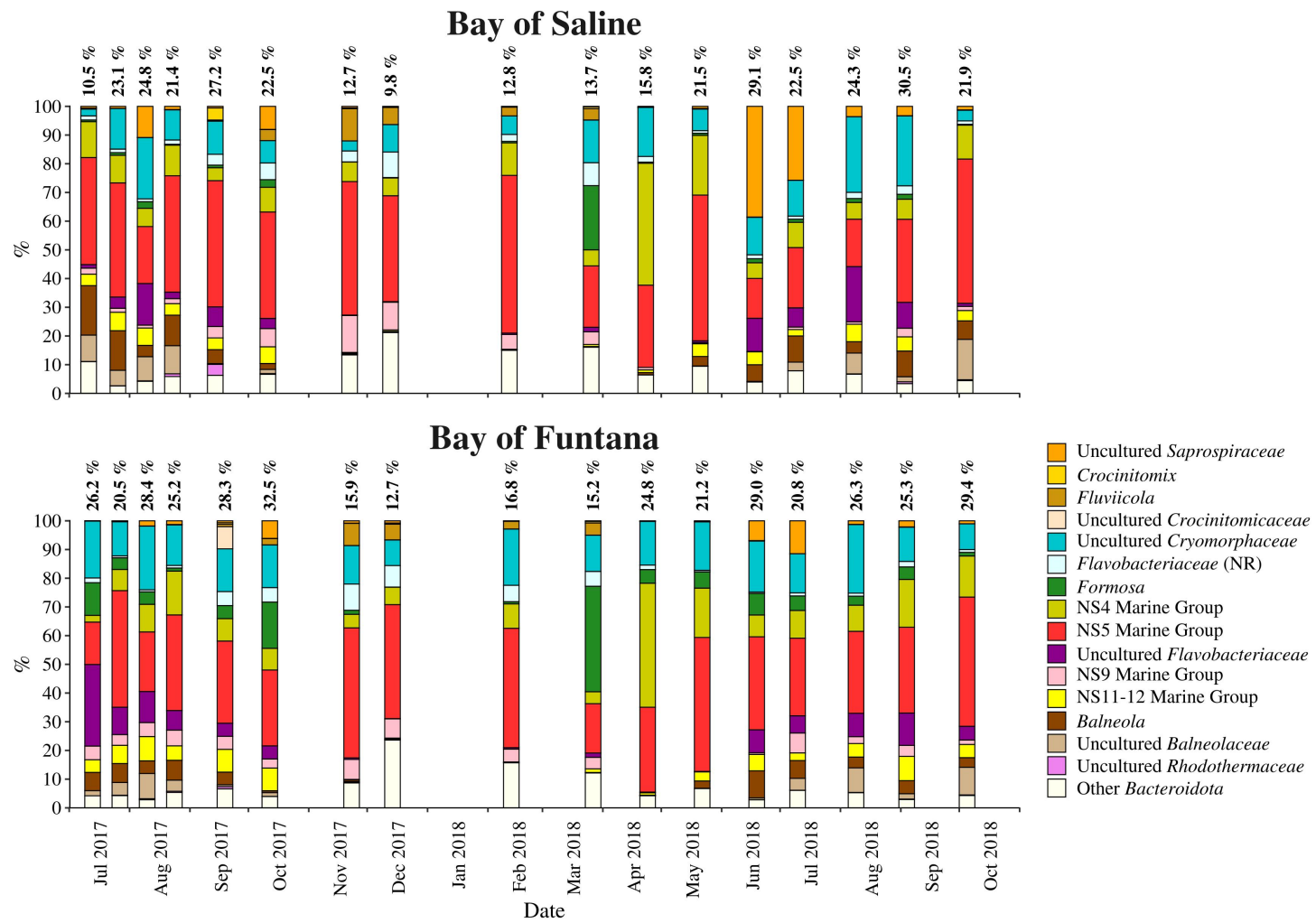


Fig. 4. Taxonomic classification and relative contribution of the most abundant ($\geq 1\%$) sequences within the *Bacteroidota* in communities sampled in Saline and Funtana Bay. The proportion of sequences classified as *Bacteroidota* in the total bacterial and archaeal community is given above the corresponding bar. NR – No Relative (sequences without known relatives within the corresponding group)

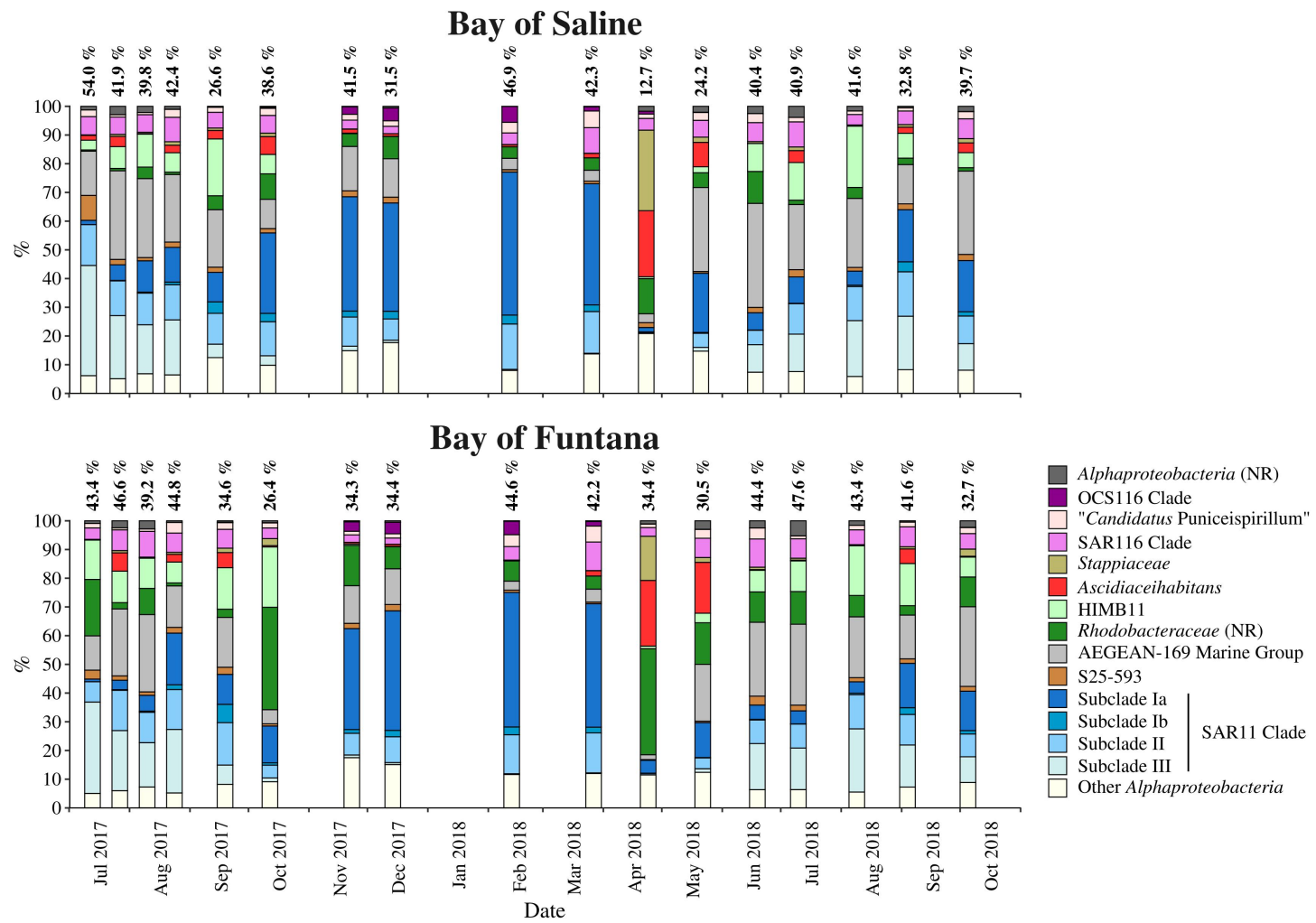


Fig. 5. Taxonomic classification and relative contribution of the most abundant ($\geq 2\%$) alphaproteobacterial sequences in communities sampled in Saline and Funtana Bay. The proportion of alphaproteobacterial sequences in the total bacterial and archaeal community is given above the corresponding bar. NR – No Relative (sequences without known relatives within the corresponding group)

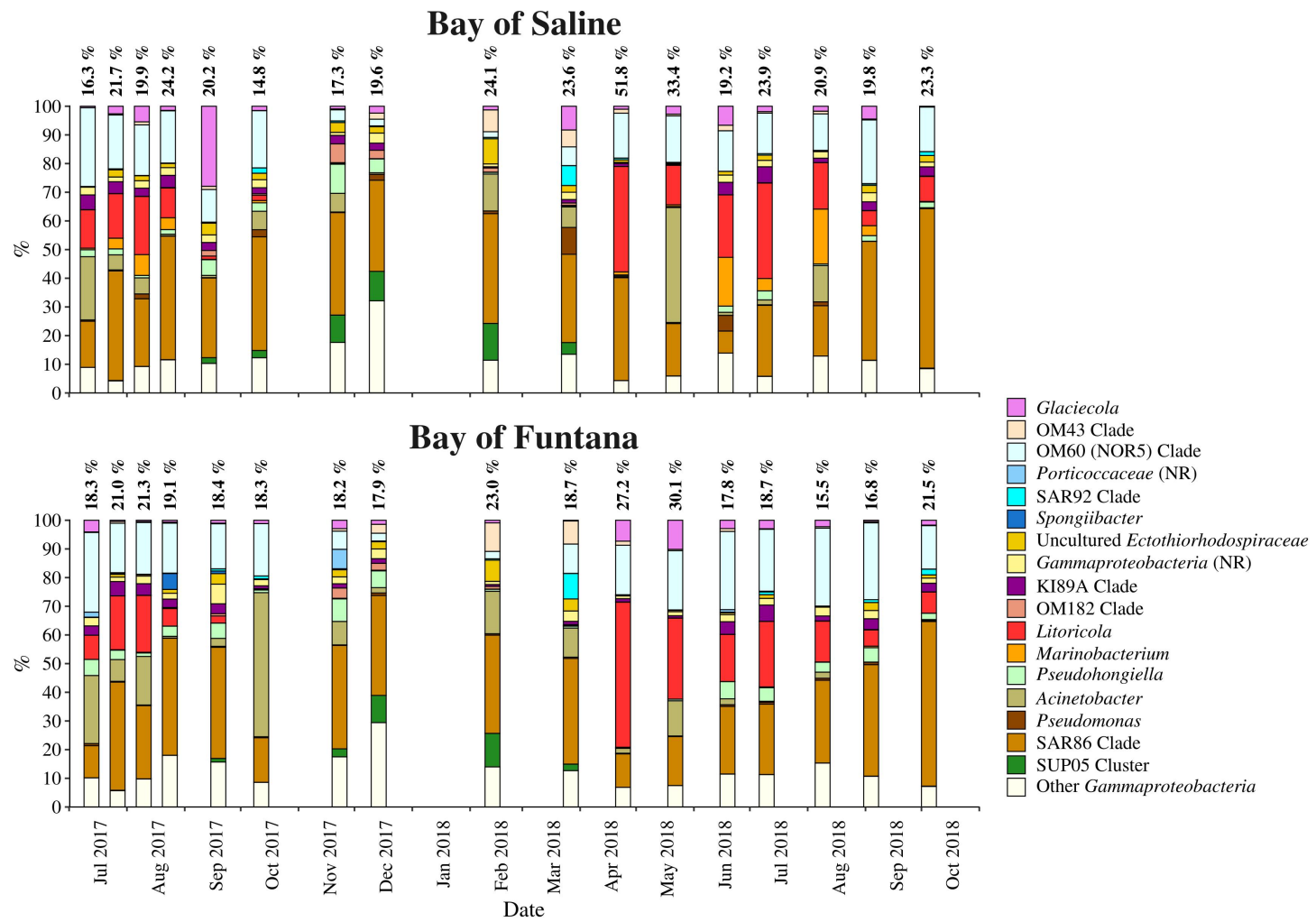


Fig. 6. Taxonomic classification and relative contribution of the most abundant ($\geq 1\%$) gammaproteobacterial sequences in communities sampled in Saline and Funtana Bay. The proportion of gammaproteobacterial sequences in the total bacterial and archaeal community is given above the corresponding bar. NR – No Relative (sequences without known relatives within the corresponding group)